Physiological
Measurement

PAPER • **OPEN ACCESS**

Validation of three-dimensional thoracic electrical impedance tomography of horses during normal and increased tidal volumes

To cite this article: David P Byrne *et al* 2024 *Physiol. Meas.* **45** 035010

IOP Publishing Physiol. Meas. 45 (2024) 035010 https://doi.org/10.1088/1361-6579/ad2eb3

Physiological Measurement

IPEM Institute of Physics and Engineering in Medicine

OPEN ACCESS

RECEIVED
22 October 2023

REVISED
7 February 2024

ACCEPTED FOR PUBLICATION
29 February 2024

PUBLISHED
21 March 2024

PAPER

Validation of three-dimensional thoracic electrical impedance tomography of horses during normal and increased tidal volumes

David P Byrne[1], Nicole Studer[2], Cristy Secombe[1], Alexander Cieslewicz[3], Giselle Hosgood[1], Anthea Raisis[1], Andy Adler[4] and Martina Mosing[5]

[1] School of Veterinary Medicine, Murdoch University, Murdoch, Western Australia, Australia
[2] Animalius, Bayswater, Western Australia, Australia
[3] Morrison Critical Care and Pulmonary, Morrison, CO, United States of America
[4] Department of Systems and Computer Engineering, Carleton University, Ottowa, ON, Canada
[5] Anaesthesia and Perioperative Intensive Care, Department of Companion Animals and Horses Vetmeduni, Vienna, Austria

E-mail: d.byrne@murdoch.edu.au

Keywords: rebreathing, reconstruction, two-plane, ventilation distribution

Abstract

Objective. Data from two-plane electrical impedance tomography (EIT) can be reconstructed into various slices of functional lung images, allowing for more complete visualisation and assessment of lung physiology in health and disease. The aim of this study was to confirm the ability of 3D EIT to visualise normal lung anatomy and physiology at rest and during increased ventilation (represented by rebreathing). *Approach*. Two-plane EIT data, using two electrode planes 20 cm apart, were collected in 20 standing sedate horses at baseline (resting) conditions, and during rebreathing. EIT data were reconstructed into 3D EIT whereby tidal impedance variation (TIV), ventilated area, and right-left and ventral-dorsal centres of ventilation (CoV_{RL} and CoV_{VD}, respectively) were calculated in cranial, middle and caudal slices of lung, from data collected using the two planes of electrodes. *Main results*. There was a significant interaction of time and slice for TIV ($p < 0.0001$) with TIV increasing during rebreathing in both caudal and middle slices. The ratio of right to left ventilated area was higher in the cranial slice, in comparison to the caudal slice ($p = 0.0002$). There were significant effects of time and slice on CoV_{VD} whereby the cranial slice was more ventrally distributed than the caudal slice ($p < 0.0009$ for the interaction). *Significance*. The distribution of ventilation in the three slices corresponds with topographical anatomy of the equine lung. This study confirms that 3D EIT can accurately represent lung anatomy and changes in ventilation distribution during rebreathing in standing sedate horses.

Introduction

Certain lung diseases occur more commonly in the superior and inferior (known as cranial and caudal, respectively, in quadrupedal animals) regions of the lungs. Examples in humans in the more cranial or superior lung fields include mediastinal lymphoma (Martelli *et al* 2015) while examples in the more caudal or inferior lung fields include lobar or bronchopneumonia (Pahal *et al* 2023). In horses, mediastinal lymphoma and bacterial pneumonias can also display similar distributions (Garber *et al* 1994, Hepworth-Warren *et al* 2022), while exercise-induced pulmonary haemorrhage (EIPH) is an additional important disease of the caudal lung field in this species (O'Callaghan *et al* 1987b). Accurate regional localisation of changes in pulmonary physiology, as well as disease, are thus important for the understanding of pathophysiologic derangements, as well as in clinical diagnosis. Given the similarities between horses and humans regarding distribution of lung pathology, as well as the large assessable volume of lung in horses, and their significant reserve capacity, horses represent a valid experimental model for this study.

Electrical impedance tomography (EIT) is a non-invasive, real-time imaging device used primarily to assess lung function under a variety of conditions (Putensen *et al* 2019, Tomicic and Cornejo 2019, Sacks *et al* 2021,

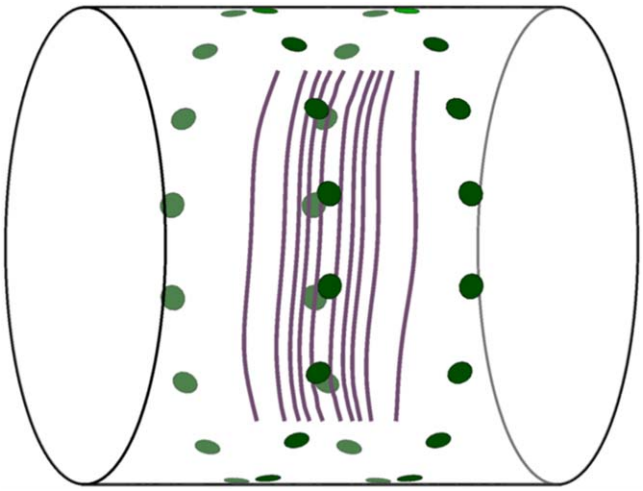

Figure 1. Illustration of single plane reconstruction and vertical sensitivity of EIT based on two electrode planes in a 'square' electrode pattern. A 'skip 4' stimulation and measurement pattern is used. A plane ¾ distance between the electrode planes is demonstrated for visual representation of the ability of two-plane EIT to reconstruct slices at any point from cranial to the cranial row of electrodes, to caudal to the caudal row of electrodes. Contour lines indicate the 99%, 95%, 90% and 80%, 50% sensitivity contours.

Secombe *et al* 2021). Typically, single-plane EIT is used where a single line of electrodes is placed around the thorax, and generates a single 2D slice with an elliptical shape in the longitudinal axis (Rabbani and Kabir 1991, Adler and Holder 2021). Single-plane EIT has been used in horses to describe changes in ventilation distribution in standing horses (Ambrisko *et al* 2016), under general anaesthesia (Ambrisko *et al* 2017, Mosing *et al* 2017, 2018, 2019), pregnancy (Schramel *et al* 2012), cardiac disease (Sacks *et al* 2021) and in naturally-occurring and experimental bronchoconstriction (Herteman *et al* 2021, Secombe *et al* 2020, 2021). Limitations of single-plane EIT include evaluation of subtotal lung volume in a longitudinal plane. In particular, cranial and caudal lung fields may be incompletely assessed, and focal or regional changes in ventilation may be missed. This is due to the vertical sensitivity of single-plane EIT typically extending to half of the diameter of the thorax cranially and caudally in the centre of the thorax, with this distance reducing towards the periphery (Brabant *et al* 2022). Increased vertical sensitivity leads to increased contributions from off-plane lung tissue, potentially leading to artefactual or erroneous reconstruction of that area. In comparison, the vertical sensitivity of slices reconstructed from two-plane EIT is smaller, leading to a more tightly constrained set of voxels contributing to slice reconstruction (figure 1), and thus increased accuracy for that particular lung region.

Two-plane EIT involves the placement of two parallel rows of electrodes around the thorax, instead of one row. This allows generation of multiple 2D slices, with more complete assessment of the thorax over a longer longitudinal axis (i.e. leading to an overall 3D assessment of the thorax). Two-plane EIT can be reconstructed into multiple slices from cranial to the cranial row of electrodes, through to caudal to the caudal row of electrodes (3D EIT). For clarification, single- or two-plane EIT refers to the electrode layout used during data collection, while 2D or 3D EIT refers to the reconstruction of a single or multiple slices during image reconstruction (Brabant *et al* 2022). Initial experience with 3D EIT image reconstruction in horses demonstrates that there is better separation between the right and left lungs than with 2D EIT, and plausible functional images of lung fields both between and outwith the two electrode planes (Grychtol *et al* 2019).

The aim of this paper was to compare the distribution of ventilation, particularly in the longitudinal axis, in standing sedated horses at baseline and increased tidal volume (rebreathing) using two-plane EIT (and subsequent 3D reconstruction) with well-defined physiologic and anatomic findings in standing horses. The objective was to describe the reconstruction of two-plane EIT into multiple planes (3D EIT), while excluding non-lung EIT signal (heart and gastrointestinal tract). The hypotheses were that distribution of ventilation would change across reconstructed plane (cranial, middle and caudal), time (baseline and rebreathing), and these changes would correspond to expected anatomy and physiology.

Materials and methods

The experiment was designed to collect two-plane EIT data from clinically healthy horses and reconstruct the data into three 2D slices (cranial, middle and caudal). In addition, given the larger volume of EIT data collected, it was intended to explore the possibility of multiplanar reconstruction of 3D EIT data. The two-plane component of the belt comprised two parallel rows of electrodes spaced 20 cm apart. Given an average thorax

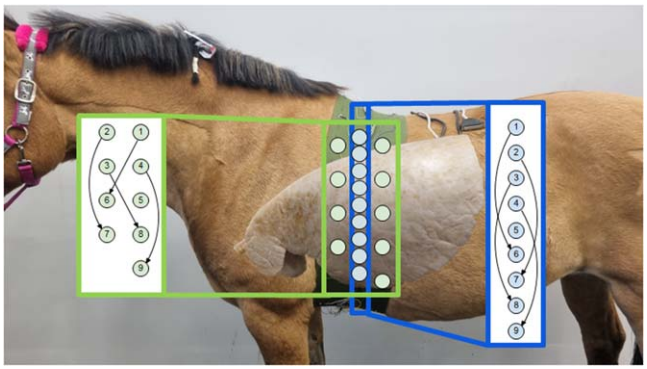

Figure 2. Combined single-plane and two-plane belt with overlaid lungs: lateral view of horse with combined single-plane and two-plane belt to demonstrate electrode position on topographical anatomy, and underlying lung anatomy. Inset left: diagrammatic representation of the skip-4 driving of electrodes in a square manner across the two planes. Inset right: diagrammatic represensation of the skip-4 driving of electrodes in the single-plane. Photo credit: Gabmaier Christopher.

height (dorsoventral measurement at the plane of the centre EIT electrode) of 80 cm, this width represents 25% of the height. The cranial row was placed immediately caudal to the elbow at the level of the 5th intercostal space. This placement was designed to capture the largest possible lung volume, with 3D EIT expected to demonstrate normal anatomic ventilatory distribution during baseline and rebreathing. Here, normal anatomic findings are considered the anatomic layout of the lungs in adult horses and the changes in lung position within the thorax from cranial to caudal—that the cranial lung is more ventrally located than the caudal lung (Nakakuki 1993). This is not expected to significantly change between conditions (baseline versus rebreathing). Physiologic norms are considered the expected changes in the distribution of ventilation observed during hyperventilation. In particular, increases in tidal volume are expected to shift proportionally more ventilation ventrally (Ambrisko *et al* 2016). In addition, rebreathing has been shown to reduce variability in measurements in pulmonary function indices, thus eliminating some physiologic factors leading to measurement error (Guthrie *et al* 1995).

Horses

As this was an exploratory study with no prior data, a sample size calculation was not able to be performed. Twenty horses were recruited from the Murdoch University School of Veterinary Medicine teaching herd. Horses were identified as clinically healthy based on history and thorough physical examinations with special focus on the respiratory tract before inclusion in the study. Several horses had mild to moderate cardiac disease: ventricular septal defects (three horses), aortic regurgitation (two horses) and tricuspid regurgitation (one horse). All horses had otherwise normal cardiac size and function at the time of the experiment, and no evidence of lung dysfunction. The horses included three mares (females) and 17 geldings (castrated males), with a mean (SD) age of 11.3 (6.3) years and bodyweight of 512 (64) kg. The median (range) body condition score was 6/9 (4–7/9) (Henneke *et al* 1983). Horses were excluded from the study if they objected strenuously to instrumentation, despite sedation. This study was part of a larger study where horses were exposed to body position changes (ramps and leg lifts) to evaluate changes in distribution of ventilation.

Experimental protocol

This study evaluated 3D EIT data collected during baseline and rebreathing arms in neutral standing positions. Each horse was walked into stocks from the paddock to which they were accustomed through regular habituation therein. An 18-gauge 4 cm intravenous catheter (Surflo, Terumo, Philippines) was placed aseptically in a jugular vein. For all data, a custom-made neoprene EIT belt was used, with 32 equidistantly mounted electrodes (for single-plane EIT data collection) and two additional rows of 16 equidistantly mounted electrodes in parallel, 20 cm apart, for two-plane EIT data collection. Each row of 16 electrodes was mounted 10 cm from the central single-plane row of 32 electrodes (figure 2). The belt was placed around the thorax with the single-plane row of electrodes at the 6th intercostal space at mid thorax, after the hair coat was circumferentially wetted with water to improve electrode contact. A small amount of non-conductive ultrasound gel was placed on each electrode prior to placement. The belt was connected to the EIT device (BBvet, SenTec AG, Landquart, Switzerland) which applied a skip-4 method of current injection to electrodes, positioned in a square configuration (figure 2). EIT data were displayed and recorded using the accompanying software (BBvet, SenTec AG, Landquart, Switzerland). For this component of the experiment, only two-plane EIT data were evaluated.

Horses were sedated with 5 μg kg^{-1} detomidine hydrochloride IV (Detomo Vet, Ceva Animal Health Pty Ltd, Glenorie, NSW, Australia). Further sedation was provided either with boluses of detomidine IV

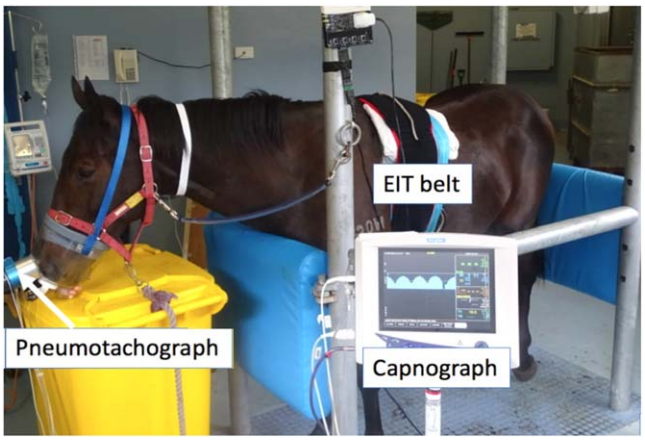

Figure 3. Experimental horse setup: sedated horse wearing two-plane EIT belt with pneumotachograph and capnograph. The expandable tubing is used to induce rebreathing, and thus an increase in tidal volume.

(2.5 μg kg^{-1}; ten horses) or a continuous rate infusion at 12.5 μg kg^{-1} h^{-1} (ten horses) for the duration of the experiment. After collection of baseline data, a face mask (Aeromask, Trudell Medical International, Ontario, Canada) was placed on the horse's muzzle and a Fleisch no. 5 pneuomotachograph connected to a commercial equine spirometry system (OpenPleth; Ambulatory

Monitoring Inc., Ardsley, NY, United States) was attached to a port on the face mask to measure airflow (figure 3). Spirometry data was recorded electronically using the included software system (Equine Flowmetrics, Ambulatory Monitoring Inc., Ardsley, NY, United States). The spirometer was calibrated with a 3L calibration syringe (Model 5630 series, Hans Rudolph Inc., Shawnee, KS, United States) prior to use on each horse. Tubing was fixed to the spirometer to increase dead space and thus increase inspired carbon dioxide, leading to an increased tidal volume and respiratory rate ('rebreathing'). Spirometry was used to measure tidal volume and confirm hyperventilation. End-tidal carbon dioxide ($EtCO_2$) was measured using a sidestream analyser connected to the spirometer (Surgivet, multiparameter monitor, Sound Veterinary Equipment, Rowville, VIC, Australia). Rebreathing was confirmed by tachypnoea or an $EtCO_2$ concentration of at least 60 mmHg. EIT data were recorded continuously during the experiment. For data evaluation, at least two minutes or ten breaths of EIT data were selected at each time period, after at least two minutes of stabilisation at steady state. Respiratory rate, tidal volume and $EtCO_2$ were also measured during rebreathing. At the end of the experiment, horses were deinstrumented and returned to the paddock.

Data analysis

Initial visualisation of the global EIT volume curve was performed in the native EIT software (Ibex, Sentec, CH-4106 Therwil BL, Switzerland). Ten representative breaths were selected for analyses and exported for reconstruction.

The selected breaths were imported into a Python (with Numpy and Scipy) environment for processing. Breathing data were smoothed with a Savitzky–Golay filter and then each dataset was partitioned into individual breaths based on identified end of exhalation phases, which is marked by a noticeable dip in the recorded impedances. Impedance data for each breath were individually normalized by subtracting a line connecting the previous and following end-expiratory point, to mitigate drift between start and end points of different breaths. Following this, an average breath waveform was computed by averaging all the individual breaths, aligned at the end-inspiratory point.

As two-plane EIT data can be reconstructed in a variety of different planes at various slice thicknesses, three representative transverse slices in the cranial, middle and caudal lung fields were selected for reconstruction. An elliptical ROI was placed on each slice to eliminate boundary artefacts such as non-lung changes in impedance or electrode movement. The ellipse was modelled on initial results of four horses and visually adjusted to incorporate the entire lung field based on prospective modelling on a further ten horses [Stüder *et al*, unpublished]. This modelling confirmed that the elliptical ROI appropriately included regions with sufficient impedance change to represent lung, without including excessive areas of low or no changes in impedance. The same elliptical ROI was applied to all slices. A functional region of interest (fROI) was subsequently applied to each slice (cranial, middle and caudal) filtering regions with signals of less than 10% of the maximum impedance such that they were excluded. This predominantly filters non-lung signal (cardiac and gastrointestinal [GIT]).

Table 1. Physiologic variables during rebreathing; RR: respiratory rate in breaths per minute, $EtCO_2$: end-tidal carbon dioxide concentration in mmHg, V_T: tidal volume in litres; SD: standard deviation.

Horse	RR	$EtCO_2$	V_T
1	17	60	14
2	15	67	17
3	16	64	20
4	14	61	22
5	28	58	13
6	16	60	25
7	18	66	16
8	16	64	21
9	15	57	21
10	25	62	21
11	17	60	20
12	18	67	17
13	29	66	14
14	16	58	22
15	22	64	22
16	14	67	28
17	14	68	26
18	16	64	19
19	16	65	26
20	22	70	19
AVERAGE	18	63	20
SD	4.4	3.6	4.1

Collected data from one horse also underwent multiplanar reconstruction in parasagittal and frontal planes, in addition to the transverse slices previously described. The purpose of the multiplanar reconstruction was to demonstrate the ability of 3D EIT to visualise changes in lung function in an anatomically correct manner.

For both timepoints (baseline and rebreathing) and all slices (cranial, middle and caudal), the following variables were measured or calculated: tidal impedance variation (TIV), ventilated area, centre of ventilation right to left (CoV_{RL}) and ventral to dorsal (CoV_{VD}) (Brabant *et al* 2022). Tidal impedance variation is expressed in arbitrary units, ventilated area as a ratio of right to left and CoV as a percentage where 0% is right or ventral.

Statistical analysis

All responses analysed were normal with failure to reject the null hypothesis of normality using the Shapiro-Wilk statistic. A two-factor general linear model was applied with time (baseline and rebreathing), slice (cranial, middle, caudal) and the interaction included as fixed effects. Where significant interaction, or main effects, at $p < 0.05$, post-hoc pair-wise comparisons of least squares means were compared against a Tukey-adjusted $p < 0.05$. All statistics were performed using SAS 9.4 (SAS Institute, Cary, NC, USA).

Results

All horses successfully completed the study protocol and were returned to the herd at the end of the experiment. The mean total experiment duration was 59 min with the mean duration for the data collection components reported here of 13 min. Respiratory rate, $EtCO_2$ and tidal volume during rebreathing are reported in table 1. Two horses reached the maximum deadspace volume without reaching predetermined criteria for rebreathing but were included due to the proximity to the criteria. There were no data missing for any horse or timepoint.

Reconstruction

Representative data for a single horse are shown in figure 4. Here the rebreathing phase is shown corresponding to an increase in respiratory rate and tidal volume. EIT images are shown in various slices for two breaths at the beginning and end of the rebreathing, illustrating the anatomical differences in the distribution of tidal volume, as well as the physiological changes (increased caudal distribution) at the larger breathing volumes.

Two-plane EIT data were successfully reconstructed into cranial, middle and caudal slices in all horses at both baseline and rebreathing timepoints. Data were also reconstructed in one horse into parasagittal and frontal planes, results of which demonstrated images consistent with normal functional anatomy of equine lungs

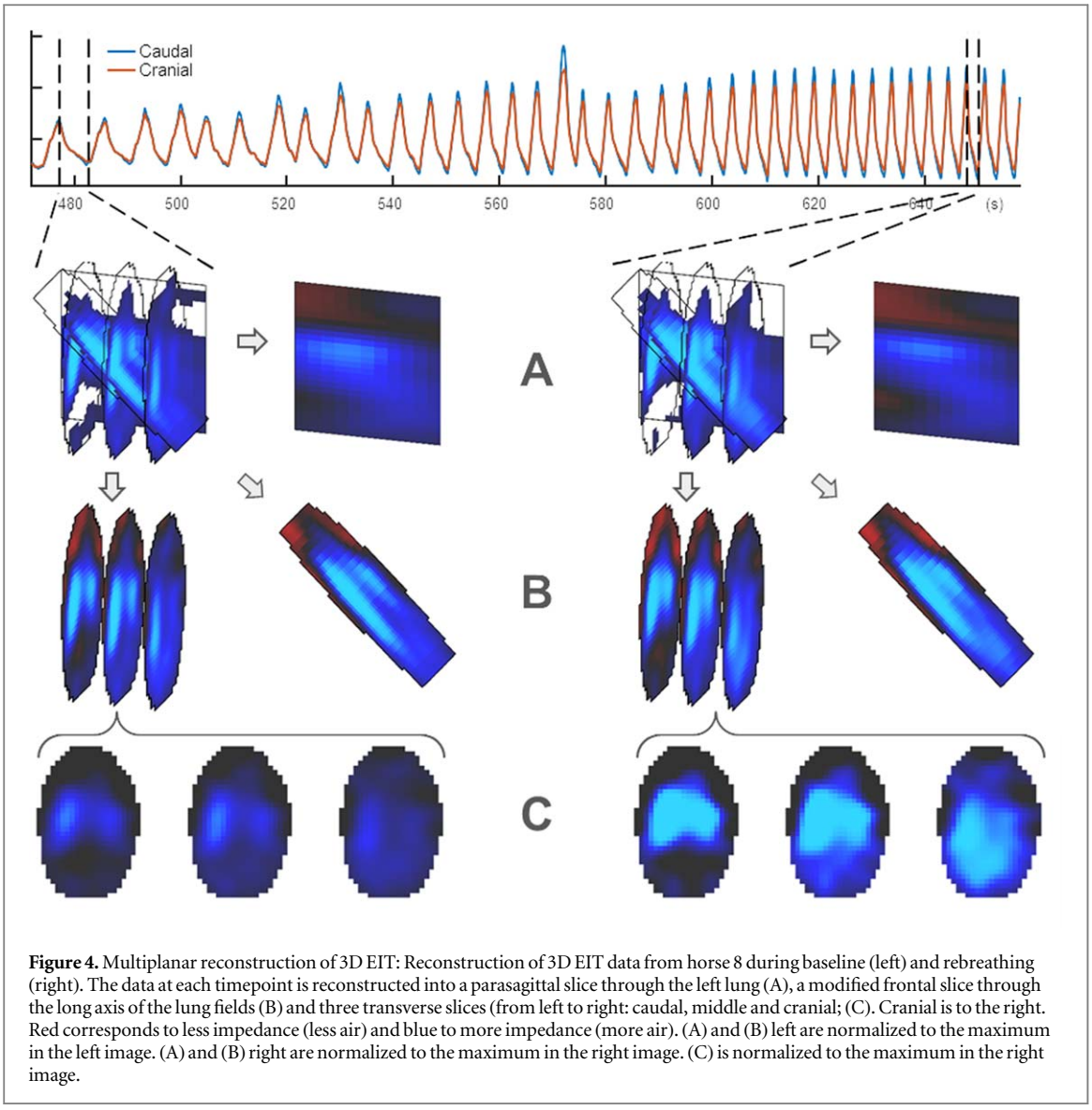

Figure 4. Multiplanar reconstruction of 3D EIT: Reconstruction of 3D EIT data from horse 8 during baseline (left) and rebreathing (right). The data at each timepoint is reconstructed into a parasagittal slice through the left lung (A), a modified frontal slice through the long axis of the lung fields (B) and three transverse slices (from left to right: caudal, middle and cranial; (C). Cranial is to the right. Red corresponds to less impedance (less air) and blue to more impedance (more air). (A) and (B) left are normalized to the maximum in the left image. (A) and (B) right are normalized to the maximum in the right image. (C) is normalized to the maximum in the right image.

(figure 4). Cardiac and gastrointestinal signals were successfully filtered out through the combination of the elliptical and functional ROIs.

Ventilation distribution

There was a significant interaction of time and slice for TIV ($p < 0.0001$) with TIV increasing during rebreathing in both caudal and middle slices. There was no significant change in TIV during rebreathing in the cranial slice (figure 5).

There was no significant effect of time or interaction of time and slice on ventilated area. There was an effect of slice whereby the ratio of right to left ventilated area was higher in the cranial slice, in comparison to the caudal slice ($p = 0.0002$; figure 6). There were no significant differences in CoV_{RL} over time or between slices ($p = 0.8879$ for the interaction; figure 7). There were significant effects of time and slice on CoV_{VD} whereby the cranial slice was more ventrally distributed than the caudal slice and ventilation moved more ventrally in the middle and caudal slices during rebreathing, but not in the cranial slice ($p < 0.0009$ for the interaction; figure 8).

Discussion

This study describes the acquisition of 3D EIT data using a two-plane EIT belt in standing, sedated horses. The distribution of ventilation in the longitudinal plane (more ventral cranially and more dorsally caudally) is consistent with lung anatomy and established ventilation distribution patterns in horse (Ambrisko *et al* 2016, O'Callaghan *et al* 1987a, Amis *et al* 1984). In addition, during rebreathing, EIT identified increased ventilation in the middle and caudal lung fields, and a more ventral distribution, the latter having previously been

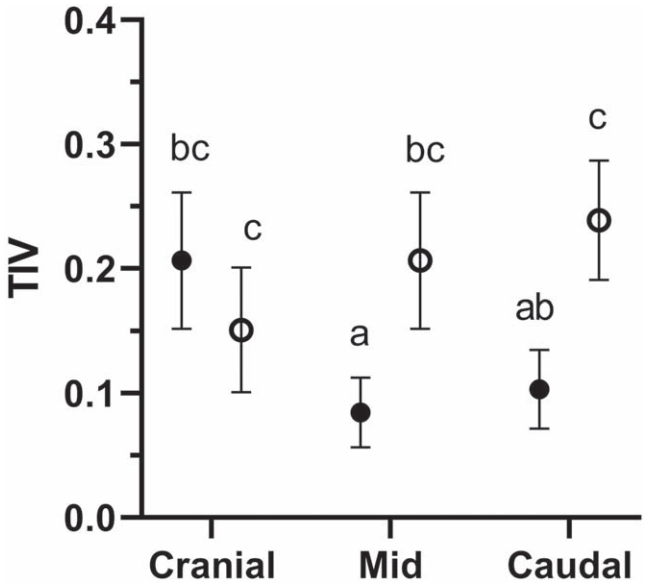

Figure 5. Interaction plot for tidal impedance variation (TIV) in arbitrary units on the *Y*-axis. Slice is on the *X*-axis. Solid dots indicate baseline conditions, open dots represent rebreathing. TIV was significantly different between baseline and rebreathing conditions for the caudal and middle slices, which were significantly different to the cranial slice ($p < 0.0001$). Different lower case letters indicate a signficant difference.

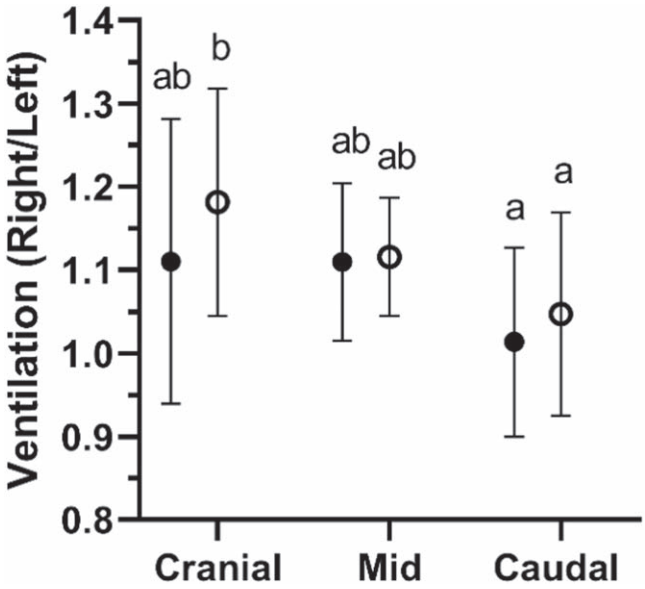

Figure 6. Interaction plot for ventilated area with the ratio of right to left ventilated area on the *y*-axis. Slice is on the *x*-axis. Solid dots indicate baseline conditions, open dots represent rebreathing. The ratio of right to left ventilated area was higher in the cranial slice, in comparison to the caudal slice ($p = 0.0002$). Different lower case letters indicate a signficant difference.

demonstrated using 2D EIT (Ambrisko *et al* 2016). Thus, 3D EIT has been shown to accurately represent normal lung anatomy and certain aspects of physiology in standing sedate horses.

The reconstruction of two-plane EIT data is more involved than the reconstruction of single-plane EIT data. In particular, consideration of reconstructed slice location involved maximising lung area and minimising non-lung signal in the slice. Slices were reconstructed cranial to the cranial row of electrodes to capture the cranial lung lobes while minimising the effects of the cardiac signal. The caudal slice was reconstructed based on lung caudal to the caudal row of electrodes (figure 2). One effect that can appear is an inverse contribution due to compression of gas in the gastrointestinal tract. Because of the sensitivity region of EIT, this effect may add to the signal in the caudal slice. It was not required to filter this effect in this study, but in general, 3D EIT offers an improved ability to reject this contribution, since it is largely isolated in caudal volumes. Interestingly, the distribution of vertical sensitivity in 3D reconstructed slices is smaller than in 'native' 2D slices collected from

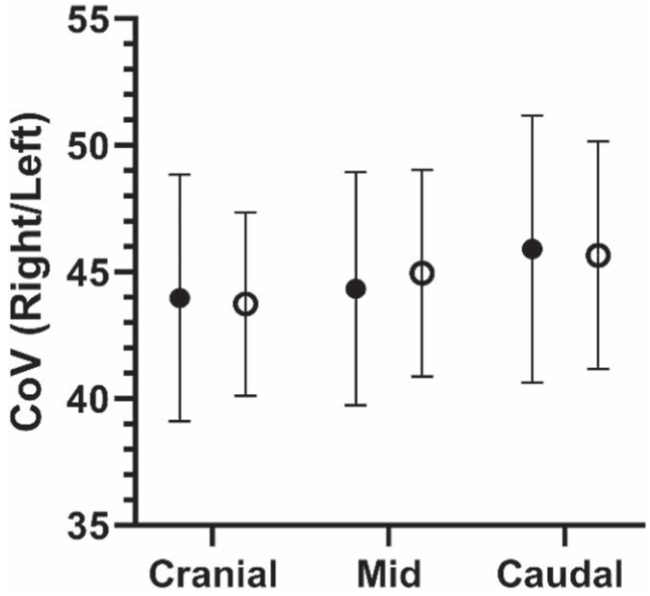

Figure 7. Interaction plot for right-to-left centre of ventilation (CoV_{RL}) with percentage on the *Y*-axis; zero is completely right ventilation. Slice is on the *X*-axis. Solid dots indicate baseline conditions, open dots represent rebreathing. There were no significant differences in CoV_{RL} over time or between slices ($p = 0.8879$).

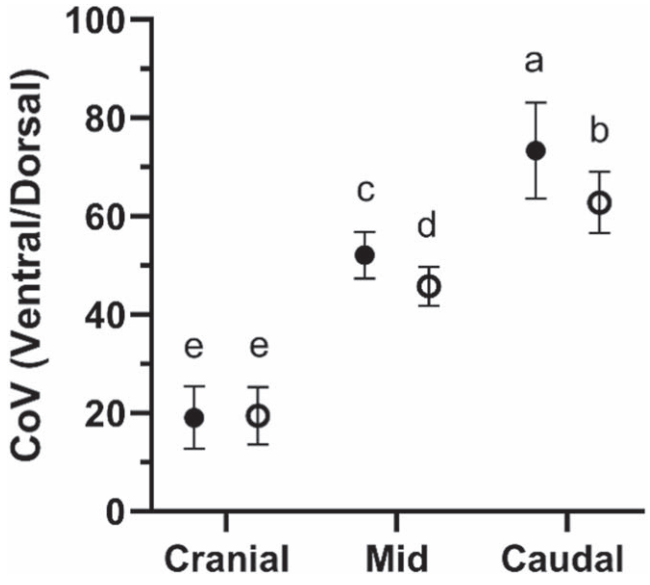

Figure 8. Interaction plot for ventrodorsal centre of ventilation (CoV_{VD}) with percentage on the *Y*-axis; zero is completely ventral ventilation. Solid dots indicate baseline conditions, open dots represent rebreathing. The cranial slice was more ventrally distributed than the caudal slice and ventilation moved more ventrally in the middle and caudal slices during rebreathing, but not in the cranial slice ($p < 0.0009$). Different lower case letters indicate a signficant difference.

single-plane belts (figure 1). Specifically, changes in impedance more cranial and caudal to a single-plane of electrodes are included in the resulting 2D slice, whereas 2D slices reconstructed from two-plane EIT results in a narrow section of lung being included in the resulting reconstructed slice. It may be that reconstructed 3D data is more appropriate and preferred for evaluation of lung disease due to fewer out-of-plane artefacts, as well as a larger assessed lung volume, particularly in heterogeneous obstructive lung disease (Young *et al* 2018).

Previous literature describing the distribution of ventilation in horses has used technetium-based radioaerosols and was able to visualise normal ventilation distribution as per anatomic norms (O'Callaghan *et al* 1987a) or to evaluate vertical gradients of ventilation (Amis *et al* 1984), comparable to CoV_{VD}. However, these techniques have not gained widespread use and EIT offers a radiation-free alternative. Other techniques evaluating regional ventilatory distribution in standing horses typically focus on changes between large, central and small, peripheral airways (Robinson *et al* 2010), or changes in ventilation in comparison with perfusion

(Hedenstierna *et al* 1987, Seaman *et al* 1995), rather than true anatomic distribution changes. The findings of this study confirm that 3D EIT visualises the distribution of ventilation in clinically healthy horses in an anatomically correct model. In particular, CoV_{VD} changed significantly from a ventral predominance in the cranial slice, to a dorsal predominance in the caudal slice, consistent with lung anatomy (figure 2).

There was a mild discrepancy between changes in ventilated area and CoV_{RL}. The ventilated area represents the proportion of the right or left side of the lung region of interest (ROI) that demonstrates changes in impedance (and thus ventilation) during breaths (Brabant *et al* 2022). In this instance, ventilated area was expressed as a ratio of right to left. The CoV_{RL}, however, is a calculated geometric mean that represents the theoretical centre of ventilation in the right to left plane (Brabant *et al* 2022). A change in ventilated area ratio from cranial to caudal (i.e. the right to left ventilated area ratio is higher in the cranial lung in comparison to the caudal lung) without an associated change in CoV_{RL} may thus represent ventilation of the accessory lung lobe or most cranial bronchus. Specifically, a preponderance (Nakakuki 1993) of larger airways in the cranial aspect of the lung fields may not lead to as much of an increase in impedance change in this area.

While forced expiratory manoeuvres are described in horses (Couëtil *et al* 2000), they are not easily achievable or frequently reported; rebreathing allows an increased tidal volume and respiratory rate which replicates physiologic hyperventilation. The results of this study revealed that ventilation moves ventrally and caudally when horses increase their tidal volume experimentally. Interestingly, TIV was higher in the cranial lung during baseline conditions, but did not significantly change during rebreathing, suggesting that horses recruit predominantly middle and caudal lung fields during rebreathing, with a concomitant shift of ventilation to more ventral lung in these areas. It should be noted that experimental rebreathing may not completely mimic causes of natural increases in tidal volume such as hypoxic drive or exercise (Lafortuna *et al* 1996).

Limitations of this study include the lack of direct anatomical comparison to the reconstructed images; data were compared to available literature on anatomy and physiology, as well as generally accepted knowledge. Generalisability and current clinical use are limited due to the lack of commercially available EIT belts for horses as well as 3D EIT algorithms. No comparisons were made with other imaging modalities (e.g. computed tomography; CT) partially due to, at the time of data collection, access to large enough equipment. In addition, while CT can determine if airflow is unlikely in a given region (e.g. atelectasis), it is more limited in evaluating distribution of ventilation, and particularly changes in this distribution with enough sensitivity.

Future research using 3D EIT can focus on reconstruction of caudal lung slices which may lead to a better understanding of diseases of the caudal lung fields, such as EIPH in horses.

Conclusion

The 3D EIT slices reconstructed from two-plane EIT were able to demonstrate expected normal lung anatomy. In addition, 3D EIT was able to evaluate ventilatory changes during rebreathing. This novel ability of 3D EIT to evaluate true anatomic regional changes, particularly in the longitudinal axis, may lead to better understanding of respiratory physiologic changes during increased ventilation (such as immediately post-exercise), as well as in disease.

Acknowledgments

The authors wish to thank Dr Jess Lynn for data evaluation and Sally McKenzie for assistance in obtaining figure 2.

Data availability statement

The data cannot be made publicly available upon publication because no suitable repository exists for hosting data in this field of study. The data that support the findings of this study are available upon reasonable request from the authors.

Funding

No funding was received for this study.

Ethical statement

This animal study was approved by Animal Ethics Committee of Murdoch University—approval: R2895/17. All animals were cared for according to the Australian code for care and use of animals for scientific purposes (https://.nhmrc.gov.au/about-us/publications/australian-code-care-and-use-animals-scientificpurposes, 2013; Accessed 23 May, 2022).

ORCID iDs

David P Byrne https://orcid.org/0000-0003-2910-9133
Cristy Secombe https://orcid.org/0000-0003-2268-1452
Giselle Hosgood https://orcid.org/0000-0002-8851-8597
Anthea Raisis https://orcid.org/0000-0002-2417-6911
Andy Adler https://orcid.org/0000-0002-2312-5346

References

Adler A and Holder D 2021 *Electrical Impedance Tomography: Methods, History and Applications* (CRC Press) (https://taylorfrancis.com/books/9780429399886)

Ambrisko T D, Schramel J, Hopster K, Kästner S and Moens Y 2017 Assessment of distribution of ventilation and regional lung compliance by electrical impedance tomography in anaesthetized horses undergoing alveolar recruitment manoeuvres *Veterinary Anaesthesia Analgesia* **44** 264–72

Ambrisko T D, Schramel J P, Adler A, Kutasi O, Makra Z and Moens Y P S 2016 Assessment of distribution of ventilation by electrical impedance tomography in standing horses *Physiol. Meas.* **37** 175–86

Amis T C, Pascoe J R and Hornof W 1984 Topographic distribution of pulmonary ventilation and perfusion in the horse *Am. J. Vet. Res.* **45** 1597–601

Brabant O A *et al* 2022 Thoracic electrical impedance tomography—the 2022 veterinary consensus statement *Front. Vet. Sci.* **9** 946911

Couëtil L L, Rosenthal F S and Simpson C M 2000 Forced expiration: a test for airflow obstruction in horses *J. Appl. Physiol.* **88** 1870–9

Garber J L, Reef V B and Reimer J M 1994 Sonographic findings in horses with mediastinal lymphosarcoma: 13 cases (1985–1992) *J. Am. Vet. Med. Assoc.* **205** 1432–6

Grychtol B, Schramel J P, Braun F, Riedel T, Auer U, Mosing M, Braun C, Waldmann A D, Böhm S H and Adler A 2019 Thoracic EIT in 3D: experiences and recommendations *Physiol. Meas.* **40** 074006

Guthrie A J, Beadle R E, Bateman R D and White C E 1995 Characterization of normal tidal breathing flow-volume loops for thoroughbred horses *Vet. Res. Commun.* **19** 331–42

Hedenstierna G, Nyman G, Kvart C and Funkquist B 1987 Ventilation-perfusion relationships in the standing horse: an inert gas elimination study *Equine Veterinary J.* **19** 514–9

Henneke D R, Potter G D, Kreider J L and Yeates B F 1983 Relationship between condition score, physical measurements and body fat percentage in mares *Equine Veterinary J.* **15** 371–2

Hepworth-Warren K L, Nelson N, Dembek K A and Young K A S 2022 Comparison of thoracic ultrasonography and thoracic radiography between healthy adult horses and horses with bacterial pneumonia using a novel, objective ultrasonographic scoring system *Front. Vet. Sci.* **9** 991634

Herteman N, Mosing M, Waldmann A D, Gerber V and Schoster A 2021 Exercise-induced airflow changes in horses with asthma measured by electrical impedance tomography *J. Vet. Intern. Med.* **35** 2500–10

Lafortuna C L, Reinach E and Saibene F 1996 The effects of locomotor-respiratory coupling on the pattern of breathing in horses *J. Physiol.* **492** 587–96

Martelli M, Di Rocco A, Russo E, Perrone S and Foà R 2015 Primary mediastinal lymphoma: diagnosis and treatment options *Expert Rev. Hematol.* **8** 173–86

Mosing M, Marly-Voquer C, MacFarlane P, Bardell D, Böhm S H, Bettschart-Wolfensberger R and Waldmann A D 2017 Regional distribution of ventilation in horses in dorsal recumbency during spontaneous and mechanical ventilation assessed by electrical impedance tomography: a case series *Veterinary Anaesthesia Analgesia* **44** 127–32

Mosing M, Auer U, MacFarlane P, Bardell D, Schramel J P, Böhm S H, Bettschart-Wolfensberger R and Waldmann A D 2018 Regional ventilation distribution and dead space in anaesthetized horses treated with and without continuous positive airway pressure: novel insights by electrical impedance tomography and volumetric capnography *Veterinary Anaesthesia Analgesia* **45** 31–40

Mosing M, Waldmann A D, Raisis A, Böhm S H, Drynan E and Wilson K 2019 Monitoring of tidal ventilation by electrical impedance tomography in anaesthetised horses *Equine Vet. J.* **51** 222–6

Nakakuki S 1993 The bronchial tree and lobular division of the horse lung *J. Vet. Med. Sci.* **55** 435–8

O'Callaghan M W, Hornof W J, Fisher P E and Rabbe O G 1987a Ventilation imaging in the horse with 99 m technetium-DTPA radioaerosol *Equine Veterinary J.* **19** 19–24

O'Callaghan M W, Pascoe J R, Tyler W S and Mason D K 1987b Exercise-induced pulmonary haemorrhage in the horse: results of a detailed clinical, post mortem and imaging study: V. Microscopic observations *Equine Veterinary J.* **19** 411–8

Pahal P, Rajasurya V and Sharma S 2023 Typical Bacterial Pneumonia *StatPearls* (StatPearls Publishing) Online: http://ncbi.nlm.nih.gov/books/NBK534295/

Putensen C, Hentze B, Muenster S and Muders T 2019 Electrical impedance tomography for cardio-pulmonary monitoring *JCM* **8** 1176

Rabbani K S and Kabir A M B H 1991 Studies on the effect of the third dimension on a two-dimensional electrical impedance tomography system *Clin. Phys. Physiol. Meas.* **12** 393–402

Robinson N E, Olszewski M A, Boehler D, Berney C, Hakala J, Matson C and Derksen F J 2010 Relationship between clinical signs and lung function in horses with recurrent airway obstruction (heaves) during a bronchodilator trial *Equine Veterinary J.* **32** 393–400

Sacks M, Byrne D P, Herteman N, Secombe C, Adler A, Hosgood G, Raisis A L and Mosing M 2021 Electrical impedance tomography to measure lung ventilation distribution in healthy horses and horses with left-sided cardiac volume overload *J. Vet. Intern. Med.* **35** 2511–23

Schramel J, Nagel C, Auer U, Palm F, Aurich C and Moens Y 2012 Distribution of ventilation in pregnant Shetland ponies measured by electrical impedance tomography *Respir. Physiol. Neurobiol.* **180** 258–62

Seaman J, Erickson B K, Kubo K, Hiraga A, Kai M, Yamaya Y and Wagner P D 1995 Exercise induced ventilation/perfusion inequality in the horse *Equine Veterinary J.* **27** 104–9

Secombe C, Adler A, Hosgood G, Raisis A and Mosing M 2021 Can bronchoconstriction and bronchodilatation in horses be detected using electrical impedance tomography? *J. Vet. Intern. Med.* **35** 2035–44

Secombe C, Waldmann A D, Hosgood G and Mosing M 2020 Evaluation of histamine-provoked changes in airflow using electrical impedance tomography in horses *Equine Vet. J.* **52** 556–63

Tomicic V and Cornejo R 2019 Lung monitoring with electrical impedance tomography: technical considerations and clinical applications *J. Thorac. Dis.* **11** 3122–35

Young H M, Guo F, Eddy R L, Maksym G and Parraga G 2018 Oscillometry and pulmonary MRI measurements of ventilation heterogeneity in obstructive lung disease: relationship to quality of life and disease control *J. Appl. Physiol.* **125** 73–85